*Particle Accelerators*, Vol. 63, pp. 1–19
Reprints available directly from the publisher
Photocopying permitted by license only



# SIMULATION OF TAIL DISTRIBUTIONS FOR KEKB

EUN-SAN KIM*

*High Energy Accelerator Research Organization (KEK), 1-1 Oho, Tsukuba, Ibaraki, 305, Japan*

*(Received 12 March 1998; In final form 7 September 1998)*

A simulation that uses a new method to obtain tail distributions in electron–positron storage rings has been applied to KEKB. This program makes it possible to investigate the tail distribution using a simple and fast simulation method and shows good agreement with solvable cases. The simulation shows beam-tail distributions due to transverse and longitudinal rare random processes. A six-dimensional beam–beam interaction is considered. The lifetime of the electron beam in KEKB due to rare random processes and beam–beam interaction is estimated to be 5 h.

*Keywords:* Colliding beams; Particle dynamics; Storage rings

## 1 INTRODUCTION

The distribution of particles in a beam can be divided into two regions: the core region at small amplitudes and the tail region at large amplitudes. The core distribution determines the luminosity and the tail distribution affects the beam lifetime and the detector background. In particular, it is important to estimate the tail distributions, which may greatly affect the background of the detectors in a colliding accelerator, such as KEKB. It is interesting to calculate the beam tails analytically which result from several processes. Since it is not always possible to obtain the beam distributions by analytical treatments, brute-force

*1 Cyclotron Load, MS 71-259, Center for Beam Physics, LBNL, Berkeley, CA 94720 USA.

tracking can be used to simulate the beam tails. However, it requires a tremendous amount of CPU time. In particular, when rare random processes contribute to beam tails, it is actually impossible to obtain results with sufficient statistics. In that case, it is desirable to investigate the beam tails by available simulation methods.

A simple and fast simulation method was proposed to obtain the beam tail due to rare random processes.[1] The simulation method investigates the beam tails caused by rare and large-amplitude processes from the core distribution. In an earlier study this method was applied to KEKB to describe tail distributions due to longitudinal rare random processes, such as beam–beam bremsstrahlung and beam–residual gas bremsstrahlung. Only a vertical kick for the case of a flat beam was then considered in the beam–beam interaction. In this study, the same simulation method was applied to KEKB in order to understand the beam tails from both transverse and longitudinal random processes. To see the effects of tails in the transverse distribution, we considered the cases of beam–residual gas scattering in the ring and Bhabha scattering at the interaction point. To obtain more realistic tails in the beam–beam interaction, the simulation included a horizontal kick as well as a vertical kick.

A comparison with a solvable model was performed in order to confirm the validity of this simulation method. For this purpose, we considered the effect of beam–residual gas scattering for the actual vacuum pressure in the ring. It has been shown that the result of this simulation method gives a good agreement with this solvable case. We can apply this simulation method to obtain beam tails in the cases of analytically unsolvable random processes. Now, the beam tails due to Bhabha scattering, including a beam–beam interaction, is the one case which cannot be solved by analytical calculations. It can be investigated using the present method. It has been shown that beam–residual gas scattering for the actual vacuum pressure and Bhabha scattering does not affect the core distribution of the beam at KEKB. Instead, these scatterings can lead to a distribution of the tail particles. In the presence of a transverse aperture, these processes lead to a steady loss of particles. The lifetime of the electron beam at KEKB will be estimated in a simulation by counting the number of the particles extending beyond the transverse aperture due to scatterings as well as the energy aperture due to bremsstrahlungs.

This paper is structured as follows: in Section 2 the simulation method is reviewed; in Section 3 the results of simulation method in the transverse distribution are checked by a comparison with an analytically solvable example. Some applications that include both longitudinal and transverse rare random processes are discussed in Section 4. Section 5 is devoted to a discussion and conclusion.

## 2 DESCRIPTION OF THE SIMULATION METHOD

This section reviews the simulation method which follows from earlier work. Suppose that an electron undergoes elastic collision with residual gas present in a vacuum chamber. We describe a method which can be used to simulate these processes and to find the equilibrium distribution.

The simulation starts with $n$ macroparticles that are given randomly with specified variances in six-dimensional phase space. Each macroparticle ($i$) has a particle number ($N_i$). Let $p$ be the probability that an electron undergoes a random process during one turn. Once an electron in a macroparticle undergoes this process (the probability $P$ is $N_i p$), we create a new macroparticle $(n+1)$th. This new macroparticle has one particle ($N_{i+1} = 1$) and the macroparticle which has undergone a random process now has a number of particles ($N_i - 1$).

We assume that the variation in the random variable due to a random process is limited to a range between a minimum and a maximum value. To obtain the variation, first, calculate the probability ($P$), and generate one uniform random number ($0 \leq x \leq 1$). If $x < P$, a random process occurs for the macroparticle. Second, generate a uniform random number ($\theta_1$) in the interval between the minimum value ($\theta_c$) and the maximum value ($\theta_m$) and one uniform random number in the interval $0 < y < (\mathrm{d}\sigma(\theta)/\mathrm{d}\theta)_{\max}$, and compare $y$ and $(\mathrm{d}\sigma(\theta)/\mathrm{d}\theta)_{\theta=\theta_1}$. Here, $\theta$ is the scattering-angle random variable and $(\mathrm{d}\sigma(\theta)/\mathrm{d}\theta)_{\theta=\theta'}$ is the cross section corresponding to $\theta'$. If $y < (\mathrm{d}\sigma(\theta)/\mathrm{d}\theta)_{\theta=\theta_1}$, a random variation corresponding to $\theta_1$ is given to an electron. If $y > (\mathrm{d}\sigma(\theta)/\mathrm{d}\theta)_{\theta=\theta_1}$, discard these $\theta_1$ and $y$, and generate new $\theta_1$ and $y$ until the relation $y < (\mathrm{d}\sigma(\theta)/\mathrm{d}\theta)_{\theta=\theta_1}$ holds.

One should find a reasonable minimum cutoff value for each of the random processes by testing several values. The choice of too small a cutoff value reduces the efficiency of this simulation, without giving any

contribution to the beam tails; and a large cutoff value can result in larger statistical fluctuations. The equilibrium beam distributions should not be affected by variations of this parameter. An example used to show this fact will be given in Section 3.1.

Here, we consider the beam distribution due to the effects of random processes which may occur in the transverse and longitudinal motions.

Each macroparticle in the simulation is tracked as follows:

1. *Input* We use the following normalized variables in tracking:

$$X = \frac{x}{\sigma_x^0}, \quad P = \frac{\beta_x^{\mathrm{IP}} P_x}{\sigma_x^0}, \quad Y = \frac{y}{\sigma_y^0}, \tag{1}$$

$$Q = \frac{\beta_y^{\mathrm{IP}} P_y}{\sigma_y^0}, \quad Z = \frac{z}{\sigma_z^0}, \quad E = \frac{\varepsilon'}{E_0 \sigma_\varepsilon^0}. \tag{2}$$

Here, the $\sigma_x^0$, $\sigma_y^0$ and $\beta^{\mathrm{IP}}$ are nominal values of the transverse beam sizes and betatron function at the interaction point, respectively. $E_0$, $\sigma_z^0$, $\sigma_\varepsilon^0$ and $\varepsilon'$ $(= E - E_0)$ are the nominal energy, nominal bunch length, relative energy spread and energy deviation due to a random process, respectively.

2. *Random process* When a longitudinal random process, such as beam–residual gas bremsstrahlung, occurs, the energy of a particle is varied by

$$E = E - \frac{\varepsilon'}{E_0 \sigma_\varepsilon^0}, \tag{3}$$

where $\varepsilon'$ is given by values between the minimum cutoff energy and the energy aperture of the beam.

When a transverse random process, such as beam–residual gas scattering, occurs, the momenta of a particle are varied by

$$P = P - \frac{\theta}{\sigma_x'}, \qquad Q = Q - \frac{\theta}{\sigma_y'}. \tag{4}$$

Here, the scattering angle $(\theta)$ is given by values between the minimum cutoff angle and the transverse aperture of the beam. $\sigma_x' = \sigma_x/\beta_x$ and $\sigma_y' = \sigma_y/\beta_y$, were, $\sigma_x$, $\sigma_y$, $\beta_x$ and $\beta_y$ are the horizontal beam size, the vertical beam size, the horizontal betatron function and vertical

betatron function at the position where the scattering process occurs, respectively.

3. *Beam–beam interaction* We consider a synchro-beam interaction:[2]

$$X = X - R_{1x} Z \delta P, \quad P = P + \delta P, \quad Y = Y - R_{1y} Z \delta Y, \quad Q = Q + \delta Q, \tag{5}$$

$$Z = Z, \quad E = E + R_{2x} \delta P (P + \delta P/2) + R_{2y} \delta Q (Q + \delta Q/2) - G_x - G_y, \tag{6}$$

$$\delta P = -\frac{\beta_x^0 f_x^{\mathrm{CP}}}{\sigma_x^0}, \quad \delta Q = -\frac{\beta_y^0 f_y^{\mathrm{CP}}}{\sigma_y^0}, \quad G_x = \frac{g_x^{\mathrm{CP}}}{\sigma_\varepsilon^0}, \tag{7}$$

$$G_y = \frac{g_y^{\mathrm{CP}}}{\sigma_\varepsilon^0}, \quad R_{1x} = \frac{\sigma_z^0}{2\beta_x^0}, \quad R_{1y} = \frac{\sigma_z^0}{2\beta_y^0}, \tag{8}$$

$$R_{2x} = \frac{1}{2\sigma_\varepsilon^0}\left(\frac{\sigma_x^0}{\beta_x^0}\right)^2, \qquad R_{2y} = \frac{1}{2\sigma_\varepsilon^0}\left(\frac{\sigma_y^0}{\beta_y^0}\right)^2, \tag{9}$$

$$x^{\mathrm{CP}} = x + \tfrac{1}{2} z P_x, \qquad y^{\mathrm{CP}} = y + \tfrac{1}{2} z P_y. \tag{10}$$

The transverse beam–beam kick is given by[3]

$$f_x + \mathrm{i} f_y = \frac{N r_{\mathrm{e}}}{\gamma} \sqrt{\frac{2\pi}{\sigma_x^2 - \sigma_y^2}} \left[ w\left( \frac{x + \mathrm{i} y}{\sqrt{2(\sigma_x^2 - \sigma_y^2)}} \right) - \exp\left( -\frac{x^2}{2\sigma_x^2} - \frac{y^2}{2\sigma_y^2} \right) w\left( \frac{\sigma_y x/\sigma_x + \mathrm{i}\sigma_x y/\sigma_y}{\sqrt{2(\sigma_x^2 - \sigma_y^2)}} \right) \right], \tag{11}$$

where $w(z)$ is a complex error function.

4. *Betatron oscillation*
5. *Synchrotron oscillation*
6. *Synchrotron radiation*

Larger arrays are required in the simulation program as the number of new macroparticles increases. On the other hand, it will be shown that new macroparticles reach their equilibrium distribution at less than two transverse damping times. An example to show this fact will be given in Section 3.1. Thus, new macroparticles are only tracked and binned for

two transverse damping times after they are produced by the random processes, although the original macroparticles are continuously tracked and binned every turn. The array sizes that are needed by this simulation can be reduced by this method, and we can perform long-term runs.

*Aperture limitations* The aperture limitations are set in our simulation by the input values of the apertures in the transverse and longitudinal directions. At each turn, the phase space positions of each particle are compared with the aperture limitations. Each particle which falls outside the apertures is eliminated from further trackings. The beam lifetime can be obtained by counting the number of such lost particles as a function of the aperture limitations. The lifetime of electron beam for KEKB will be estimated as a function of the transverse and longitudinal apertures.

## 3 CHECKING THE METHOD BY SOLVABLE MODELS

To show the validity of the simulation method, we compared the results of a simulation with those of the solvable model. For this purpose, we used the model of Ref. 4. The distribution function in the transverse direction is given by

$$\rho(X) = \frac{1}{\pi}\int \mathrm{d}K \cos(KX) \exp\left[-\frac{K^2}{2} + N\tau_{\mathrm{t}}\hat{f}\left(\frac{K}{\sigma_0'}\right)\right], \tag{12}$$

which is normalized to unity, $\int \rho(X)\,\mathrm{d}X = 1$ and $\tau_{\mathrm{t}}$ is the transverse damping time. $\sigma_0' = \sigma_0/\beta$ is the nominal betatron rms beam size. $N$ is the number of times that a particle undergoes random processes per unit time. $X$ denotes the one-dimensional direction.

The distribution function in the longitudinal distribution is given by[1]

$$\rho(E) = \frac{1}{\pi}\int \mathrm{d}K \cos(KE) \exp\left[-\frac{K^2}{2} + \frac{N\tau_\varepsilon}{2}\hat{f}\left(\frac{K}{E_0\sigma_\epsilon^0}\right)\right], \tag{13}$$

which is normalized to unity, $\int \rho(E)\,\mathrm{d}E = 1$. $\tau_\varepsilon$ is the longitudinal damping time.

A weak–strong simulation was performed with 40 000 macroparticles that were Gaussain distributed in six-dimensional phase space.

TABLE I Main parameters in KEKB

| *Parameter* | | *LER* | *HER* |
|---|---|---|---|
| Energy | $E$ (GeV) | 3.5 | 8.0 |
| Circumference | $C$ (m) | 3016.26 | 3016.26 |
| Beta function at IP | $\beta_x$ (m)/$\beta_y$ (m) | 0.33/0.01 | 0.33/0.01 |
| Natural bunch length | $\sigma_z$ (cm) | 0.4 | 0.4 |
| Energy spread | $\sigma_\epsilon$ | $7.1 \times 10^{-4}$ | $6.7 \times 10^{-4}$ |
| Particles/bunch | $N$ | $3.3 \times 10^{10}$ | $1.4 \times 10^{10}$ |
| Beam current | $I(A)$ | 2.6 | 1.1 |
| Betatron tune | $\nu_x/\nu_y$ | 45.54/45.08 | 47.52/43.08 |
| Synchrotron tune | $\nu_s$ | 0.01–0.02 | 0.01–0.02 |
| Emittance | $\epsilon_x$ ($10^{-8}$ m)/$\epsilon_y$($10^{-10}$m) | 1.8/3.6 | 1.8/3.6 |
| Tune shifts | $\xi_x/\xi_y$ | 0.039/0.052 | 0.039/0.052 |
| Longitudinal damping time | $\tau_\epsilon$ (ms) | 23 | 23 |

The results of a simulation for the design parameters of KEKB were obtained. The parameters are listed in Table I.[5]

### 3.1 Beam–Residual Gas Scattering

The deflection of an electron via a Coulomb interaction is described by Rutherford scattering. We assume that this scattering is elastic and that the recoil momemtum of the residual gas is negligible. The initial and final energies of the electron are therefore the same. The cross section of the elastic scattering with an atom is given by[6]

$$\frac{d\sigma}{d\Omega} = \left(\frac{2Zr_e}{\gamma}\right)^2 \frac{1}{(\theta^2 + \theta_{min}^2)^2}, \tag{14}$$

where $\Omega$ is the solid angle, $\theta$ the scattering angle, $Z$ the atomic number, $r_e$ the classical electron radius and $\gamma$ the Lorentz factor; screening of the atomic electrons is accounted by the angle $\theta_{min}$, which is determined by the uncertainty principle as

$$\theta_{min} = Z^{1/3}\alpha/\gamma, \tag{15}$$

where $\alpha$ is the fine-structure constant. If we consider the scattering occurring between angle $\theta_a$ and angle $\theta_b$ in betatron phase space, we obtain

$$\sigma = 2\pi\left(\frac{2Zr_e}{\gamma}\right)^2 \left[\frac{1}{2(\theta_a^2 + \theta_{min}^2)} - \frac{1}{2(\theta_b^2 + \theta_{min}^2)}\right]. \tag{16}$$

For elastic scattering, we assume that there is only one type of molecule, so that the number of scatterings per unit time is

$$N = Q\sigma c. \tag{17}$$

Here, $c$ is the light velocity and $Q$ is the number of gas molecules in a unit volume, which is given by

$$Q = 2.65 \times 10^{20} n P_{\mathrm{a}}, \tag{18}$$

where $n$ is the number of atoms in a gas molecule and $P_{\mathrm{a}}$ is the partial pressure of the gas in pascals.

The scattering angle when a particle undergoes scattering can be obtained as follows. First, calculate the probability ($P$) that it is scattered at higher angles ($\theta$) than the minimum scattering angle ($\theta_{\mathrm{a}}$), and generate one uniform random number ($0 \leq x \leq 1$) each turn to determine whether the scattering occurs or not. If $x < P$, the scattering angle is defined by

$$\theta = \theta_{\mathrm{a}}/\sqrt{R}, \tag{19}$$

where $R$ ($0 < R < 1$) is the other uniform random number.

The scattering cross section becomes $8.88 \times 10^{-27}\,\mathrm{m}^2$ when the minimum cutoff momentum change in a particle due to the scattering is set to $8\sigma_y'$ radians, where $\sigma_y' = \sigma_y/\beta_y$. The probability that an electron scatters with residual gas during one damping time is given by

$$N_{\mathrm{BGS}} = N\tau, \tag{20}$$

where $\tau$ is the transverse damping time. We then obtain an $N_{\mathrm{BGS}}$ corresponding to $8.512 \times 10^{-9}$ for $\tau = 4600$ and $P_{\mathrm{a}} = 10^{-9}$ Torr.

Figure 1 shows the vertical distribution produced from tracking of the beam–residual gas scattering, betatron oscillation, synchrotron oscillation and synchrotron radiation. It is obtained when the vertical aperture of a particle is assumed to be $30\sigma_y^{0\prime}$ at IP, where $\sigma_y^{0\prime} = \sigma_y^0/\beta_y^{\mathrm{IP}}$. The average $\beta_y$ value at the position where the scattering occurs is set to 10 m. The dotted lines that are drawn based on the simulation show the distribution in the equilibrium state. The square symbols show the equilibrium distribution obtained from the solvable model. It is shown

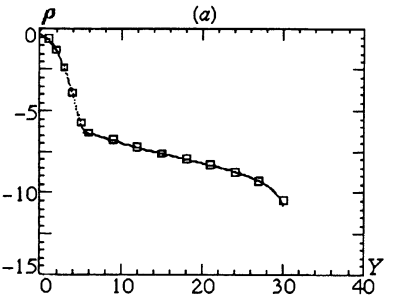


FIGURE 1 Vertical distribution from the tracking of beam–residual gas scattering, betatron oscillation, synchrotron oscillation and synchrotron radiation. The horizontal axis is $Y$, the distance normalized by the nominal vertical beam size. The vertical axis represents the distribution in $Y$ measured using a logarithmic scale. The numbers of initial macropartices and turns are 40 000 and 46 000. $\tau_\varepsilon = 2300$, $\tau_x = 4600$, $\tau_y = 4600$, $\nu_s = 0.01$, $\nu_x = 47.52$ and $\nu_y = 43.08$.

from Figure 1 that the result obtained from the simulation shows good agreement with that of the solvable model.

On the other hand, beam–residual gas scattering causes changes in the momenta of a particle in the horizontal and vertical directions. Then, the third random number is used to define the azimuthal angle ($\phi$) which is the angle between the horizontal and scattering planes. To obtain the changes in the momenta due to the scattering in terms of the normalized momenta, we have to multiply $\theta_x = \theta \cos\phi$ and $\theta_y = \theta \sin\phi$ by the value $\beta_x/\sigma_x$ and $\beta_y/\sigma_y$, respectively, taken at the position where the scattering takes place. We used 10 m as the average values of $\beta_x$ and $\beta_y$ in the ring. It thus follows that the vertical distribution of a beam is more affected than the horizontal distribution by the beam–residual gas scattering due to the relation $\beta_y/\sigma_y > \beta_x/\sigma_x$. Figure 2(a) and (b) shows the horizontal and vertical distributions due to the beam–residual gas scattering for a vacuum of $10^{-9}$ Torr. The minimum cutoff momentum change in a particle due to scattering is set to $8\sigma'_y$ radian, as in the case of Figure 1. The horizontal and the vertical apertures of a particle are set to $34\sigma_x^{0\prime}$ radian and $30\sigma_y^{0\prime}$ radian at IP, respectively, where $\sigma_x^{0\prime} = \sigma_x^0/\beta_x^{\mathrm{IP}}$. The vertical distribution of Figure 2 shows a lower density distribution in the tail by the factor $\cos\phi$ than that of Figure 1. It is shown from the Figure 2(a) and (b) that particle losses due to beam–residual gas scattering in KEKB are mainly limited by the vertical aperture.

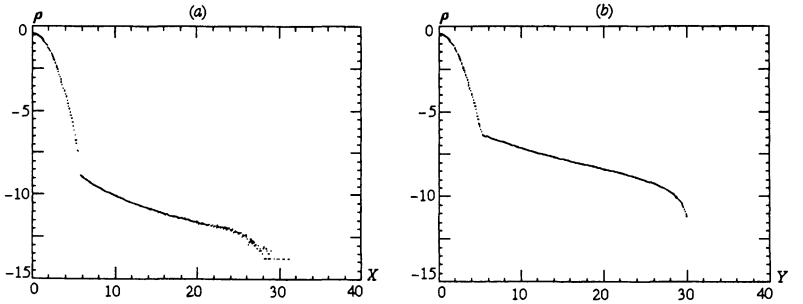


FIGURE 2 (a) Horizontal and (b) vertical distributions from the tracking of beam–residual gas scattering, betatron oscillation, synchrotron oscillation and synchrotron radiation. When an electron undergoes scattering by a deflection of $\theta$, the changes of its trajectory in the horizontal and vertical directions are given by $\theta_x = \theta \cos\phi$ and $\theta_y = \theta \sin\phi$, respectively. The horizontal axes are $X$, the distance normalized by the nominal horizontal beam size, and $Y$, the distance normalized by the nominal vertical beam size. The vertical axes represent the distributions in $X$ or $Y$ measured using the logarithmic scale. The number of initial macropartices and turns are 40 000 and 46 000. $\tau_\varepsilon = 2300$, $\tau_x = 4600$, $\tau_y = 4600$, $\nu_s = 0.01$, $\nu_x = 47.52$ and $\nu_y = 43.08$.

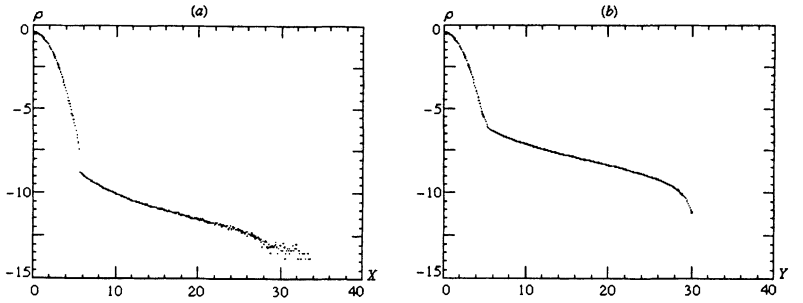


FIGURE 3 (a) Horizontal and (b) vertical distributions from the tracking of beam–residual gas scattering, betatron oscillation, synchrotron oscillation and synchrotron radiation when the minimum cutoff momentum is set to $4\sigma'_y$. The horizontal axes are $X$, the distance normalized by the nominal horizontal beam size, and $Y$, the distance normalized by the nominal vertical beam size. The vertical axes represent the distributions in $X$ or $Y$ measured using the logarithmic scale. The number of initial macropartices and turns are 40 000 and 46 000. $\tau_\varepsilon = 2300$, $\tau_x = 4600$, $\tau_y = 4600$, $\nu_s = 0.01$, $\nu_x = 47.52$ and $\nu_y = 43.08$.

Figure 3(a) and (b) shows the horizontal and vertical distributions when the minimum cutoff momentum is $4\sigma'_y$ radian. They show almost the same distribution as in Figure 2(a) and (b) in which the minimum cutoff momentum is $8\sigma'_y$ radian. This shows an example that the $8\sigma'_y$

which is used in our simulation is reasonable as the minimum cutoff momentum.

Figure 4(a) and (b) shows the horizontal and vertical distributions after ten transverse damping times for tracking of the beam–residual gas scattering, betatron oscillation, synchrotron oscillation and synchrotron radiation. Figure 4(a) and (b) shows the distributions for the case that new macroparticles are continuously tracked after their production. On the other hand, Figure 2(a) and (b) shows the distributions for the case that new macroparticles are only tracked during two transverse damping times after their production. This comparison shows a good agreement. The method by which new macroparticles are tracked for two transverse damping times can solve the problem for the large arrays needed due to an increasing number of new macroparticles. This makes it possible to reduce the amount of CPU time and to run a long-term simulation.

It is also shown that the core and tail parts of the distribution are smoothly connected as the number of turns increases. This means that the tail parts which leave the core due to scatterings dampen back toward the core part.

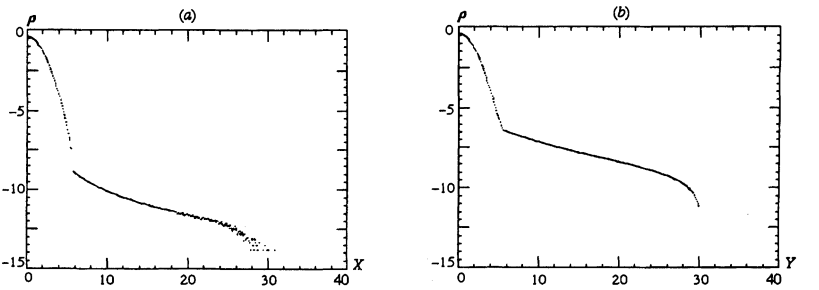


FIGURE 4 (a) Horizontal and (b) vertical distribution after ten transverse damping times from the tracking of beam–residual gas scattering, betatron oscillation, synchrotron oscillation and synchrotron radiation. The horizontal axes are $X$, the distance normalized by the nominal horizontal beam size, and $Y$, the distance normalized by the nominal vertical beam size. The vertical axes represent the distributions in $X$ or $Y$ measured using the logarithmic scale. The number of initial macropartices and turns are 40 000 and 46 000. $\tau_\varepsilon = 2300$, $\tau_x = 4600$, $\tau_y = 4600$, $\nu_s = 0.01$, $\nu_x = 47.52$ and $\nu_y = 43.08$.

# 4 APPLICATION

## 4.1 Random Processes in Transverse Motion

### *4.1.1 Bhabha Scattering*

The two graphs which contribute to electron–positron elastic scattering (Bhabha scattering) are shown in Figure 5. In terms of the cms scattering angle ($\theta$) of the electron, the differential cross section is given by[7]

$$\frac{d\sigma}{d\Omega} = \frac{\alpha^2}{8E_1E_2}\left[\frac{1+\cos^4\theta/2}{\sin^4\theta/2} + \frac{1+\cos^2\theta}{2} - \frac{2\cos^4\theta/2}{\sin^2\theta/2}\right], \tag{21}$$

where $\alpha$ is the fine-structure constant; $E_1$ and $E_2$ are the electron and positron energies, respectively. Note that the scattering angle is measured in the laboratory system, while the Bhabha cross section is evaluated in the center of mass system. Accordingly, in order to obtain the scattering angle in the center of mass system, we have to perform a Lorentz transformation of the momemtum and energy of a particle from laboratory system to the center of mass system. Figure 6(a) and (b) shows the horizontal and vertical distributions produced from the tracking of Bhabha scattering, betatron oscillation, synchrotron oscillation and synchrotron radiation, respectively. Here, the minimum deflections in the transverse momentum by the scattering are set to $1\sigma_y^{0\prime}$. The horizontal and vertical aperture limitations are set to $34\sigma_x^{0\prime}$ and $30\sigma_y^{0\prime}$ at IP, respectively. It is shown that Bhabha scattering does not contribute to the beam tails more than does beam–residual gas scattering.

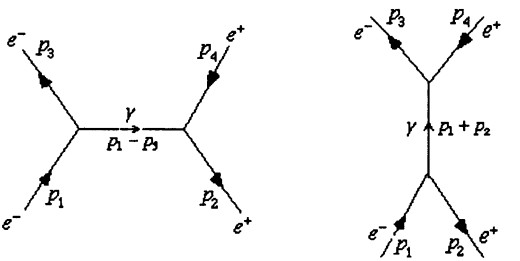


FIGURE 5 Two diagrams for $e^-e^+ \to e^-e^+$ (Bhabha scattering).

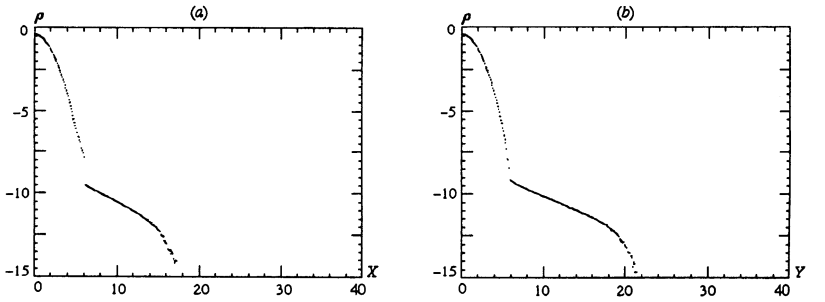


FIGURE 6 (a) Horizontal and (b) vertical distributions for the tracking of Bhabha scattering, betatron oscillation, synchrotron oscillation and synchrotron radiation. The horizontal axes are $X$, the distance normalized by the nominal horizontal beam size, and $Y$, the distance normalized by the nominal vertical beam size. The vertical axes represent the distributions in $X$ or $Y$ measured using the logarithmic scale. The number of initial macroparticles and turns are 40 000 and 312 800, respectively. $\tau_\varepsilon = 2300$, $\tau_x = 4600$, $\tau_y = 4600$, $\nu_s = 0.01$, $\nu_x = 47.52$ and $\nu_y = 43.08$.

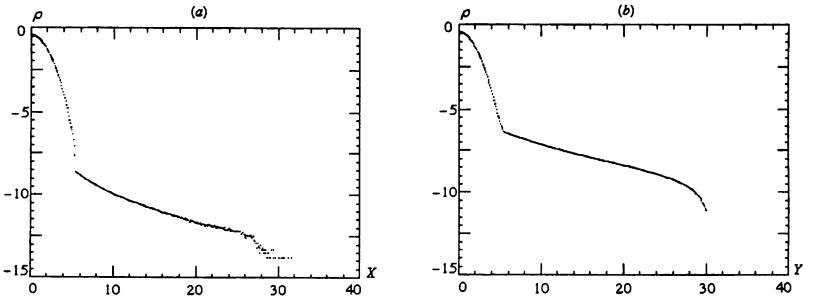


FIGURE 7 (a) Horizontal and (b) vertical distributions for a beam–beam interaction, beam–residual gas scattering, betatron oscillation, synchrotron oscillation and synchrotron radiation after 46 000 turns. The horizontal axes are $X$, the distance normalized by the nominal horizontal beam size, and $Y$, the distance normalized by the nominal vertical beam size. The vertical axes represent the distributions in $X$ or $Y$ measured using the logarithmic scale. The number of initial macroparticles is 40 000. $\tau_\varepsilon = 2300$, $\tau_x = 4600$, $\tau_y = 4600$, $\nu_s = 0.01$, $\nu_x = 47.52$ and $\nu_y = 43.02$.

### *4.1.2 Beam–Residual Gas Scattering and Bhabha Scattering*

Figure 7(a) and (b) shows the horizontal and vertical distributions produced from the tracking of Bhabha scattering, beam–residual gas scattering for a pressure of $10^{-9}$ Torr, betatron oscillation, synchrotron oscillation and synchrotron radiation. Figure 7(a) and (b) shows almost

the same distributions as Figure 2(a) and (b), in which Bhabha scattering is not included.

### *4.1.3 Beam–Residual Gas Scattering and Beam–Beam Interaction*

Figure 8(a) and (b) shows the horizontal and vertical distributions produced from the tracking of beam–beam interaction, beam–residual gas scattering for a pressure of $10^{-9}$ Torr, betatron oscillation, synchrotron oscillation and synchrotron radiation. The six-dimensional beam–beam interaction is considered.

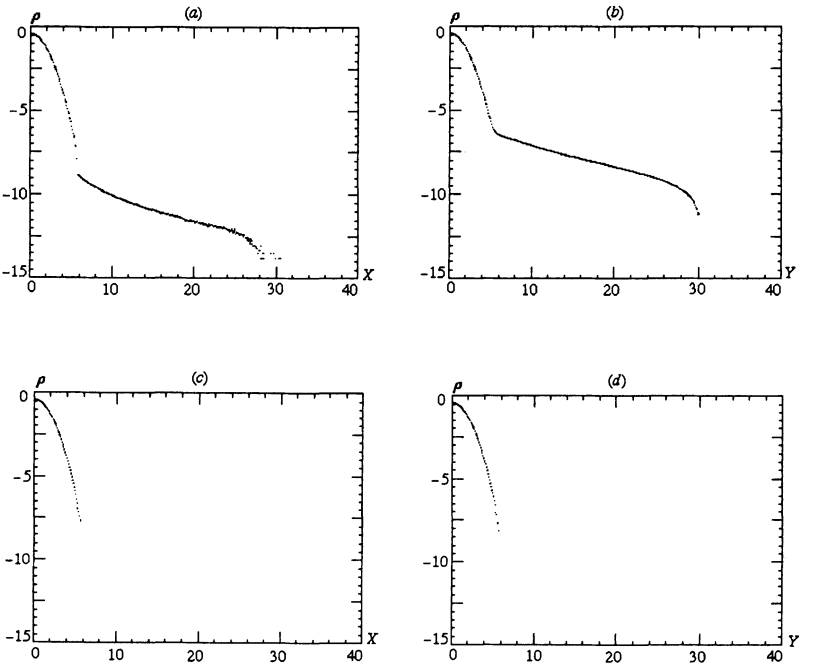


FIGURE 8 (a) Horizontal and (b) vertical distributions for the beam–beam interaction, beam–residual gas scattering, betatron oscillation, synchrotron oscillation and synchrotron radiation after 46 000 turns. (c) and (d) are the horizontal and vertical distributions after $1.288 \times 10^7$ turns when the beam–residual gas scattering is not included in (a) and (b), respectively. The horizontal axes are $X$, the distance normalized by the nominal horizontal beam size, and $Y$, the distance normalized by the nominal vertical beam size. The vertical axes represent the distributions in $X$ or $Y$ measured using the logarithmic scale. The number of initial macroparticles is 40 000 in (a) and (b) and 400 in (c) and (d). $\tau_\varepsilon = 2300$, $\tau_x = 4600$, $\tau_y = 4600$, $\nu_s = 0.01$, $\nu_x = 47.52$ and $\nu_y = 43.08$.

Figure 8(a) and (b) shows almost the same distributions as Figure 2(a) and (b), in which beam–beam interaction is not included. However, it is shown that particle losses are more increased by the beam–beam interaction. The beam lifetimes due to the rare processes and beam–beam interaction are estimated in Section 5.

Figure 8(c) and (d) shows the horizontal and vertical distributions after $1.288 \times 10^7$ turns when the beam–residual gas scattering is not included in (a) and (b), respectively. The diagrams show that the horizontal and vertical tails are caused by the beam–residual gas scattering rather than the beam–beam interaction. Accordingly, it shows one case that the beam–beam interaction dominates at small amplitudes, while the beam–residual gas scattering dominates at large amplitudes.

### 4.2 Random Processes in Longitudinal and Transverse Motions

Figure 9(a)–(c) shows the horizontal, vertical and longitudinal distributions produced from the tracking of Bhabha scattering, beam–beam bremsstrahlung, beam–beam interaction, beam–residual gas scattering for a pressure of $10^{-9}$ Torr, beam–residual gas bremsstrahlung, betatron oscillation, synchrotron oscillation and synchrotron radiation. The six-dimensional beam–beam interaction is considered. The apertures are limited by $34\sigma_x^{0\prime}$, $30\sigma_y^{0\prime}$ and $E = 15$ in the horizontal, the vertical and the energy directions, respectively. We see that particle losses in KEKB are mainly limited by the energy and the vertical apertures.

### 4.3 Lifetimes of the Electron Beam in KEKB

In this section we discuss dependence of the lifetime of the electron beam for KEKB on random processes. In KEKB, the designed apertures in the horizontal, vertical and energy directions are given by $34\sigma_x^0/\beta_x^{\mathrm{IP}}$, $30\sigma_y^0/\beta_y^{\mathrm{IP}}$ and $E = 15$, respectively. We estimated the variance of the lifetimes close to these designed apertures. Once a particle's amplitude exceeds an aperture, this particle would be lost. The lost particles are counted at one position of the ring per turn by comparing the amplitudes of the particle with the apertures. The beam lifetime is defined by

$$\tau = \frac{N}{-(\mathrm{d}N/\mathrm{d}t)}, \tag{22}$$

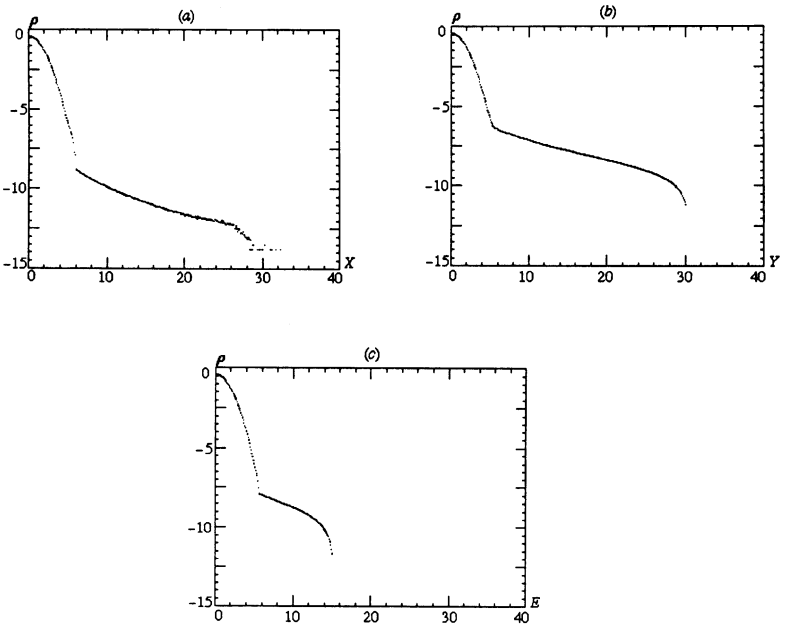


FIGURE 9 (a) Horizontal, (b) vertical and (c) longitudinal distributions for the tracking of Bhabha scattering, beam–beam bremsstrahlung, beam–beam interaction, beam–residual gas scattering, beam–residual gas bremsstrahlung, betatron oscillation, synchrotron oscillation and synchrotron radiation after 46 000 turns. The horizontal axes are $X$, the distance normalized by the nominal horizontal beam size, $Y$, the distance normalized by the nominal vertical beam size and $E$, the energy deviation normalized by the relative energy spread. The vertical axes represent the distributions in $X$, $Y$ and $E$ measured using the logarithmic scale. The number of initial macroparticles is 40 000. $\tau_\varepsilon = 2300$, $\tau_x = 4600$, $\tau_y = 4600$, $\nu_s = 0.01$, $\nu_x = 47.52$ and $\nu_y = 43.08$.

where $N$ is the initial number of particles in a beam and $-\mathrm{d}N/\mathrm{d}t$ is the total number of particles that exceed the apertures.

We consider four random processes that can lead to particle losses for a electron beam: beam–residual gas scattering and beam–residual bremsstrahlung for the single beam, and beam–beam bremsstrahlung and Bhabha scattering for two beams in collision. In our simulation average $\beta$ ($= 10$ m) instead of $\beta$(s) in the ring is used when we estimate the lifetimes due to residual gas. We used $1.0 \times 10^{-9}$ Torr which is the pressure-level goal to achieve at KEKB in the presence of the beam.

Table II gives the lifetimes that result from the scatterings as a function of the vertical apertures. The lifetimes were obtained when the

TABLE II Lifetimes due to the scatterings in KEKB

| *Vertical aperture* | $25\sigma_y^0/\beta_y^{IP}$ | $30\sigma_y^0/\beta_y^{IP}$ | $35\sigma_y^0/\beta_y^{IP}$ |
|---|---|---|---|
| Bhabha scattering | 13 182 h | 18 595 h | 25 252 h |
| Beam–residual gas scattering | 21.8 h | 31.3 h | 42.7 h |

TABLE III Lifetimes due to bremsstrahlungs in KEKB

| *Energy aperture* | $E=10$ | $E=15$ | $E=20$ |
|---|---|---|---|
| Beam–beam bremsstrahlung | 6.6 h | 7.3 h | 7.8 h |
| Beam–residual gas bremsstrahlung | 32.4 h | 35.3 h | 37.7 h |

horizontal and the energy apertures were set to $34\sigma_x^{0\prime}$ and $E=15$ at IP, respectively.

Table III gives the lifetimes due to the bremsstrahlungs as a function of the energy apertures. The lifetimes were obtained when the horizontal and vertical apertures were set to $34\sigma_x^{0\prime}$ and $30\sigma_y^{0\prime}$ at IP, respectively. In the case of an energy aperture corresponding to 1% ($E=15$) of the nominal beam energy, the lifetime due to the beam–beam bremsstrahlung was estimated to be around 7.3 h.

It was shown that particle losses due to beam–beam bremsstrahlung play an important role in the lifetime of the electron beam of KEKB. The beam–residual gas scattering and the beam–residual gas bremsstrahlung affect to the beam lifetime in order. The effect of Bhabha scattering on the beam lifetime is not as important as the other random processes considered. We have found that beam lifetimes are greatly affected by the variance in the apertures near to the designed vertical aperture.

When we estimated the lifetime due to the beam–beam interaction and random processes, it gave a lifetime of around 5 h in the aperture limitations of $34\sigma_x^{0\prime}$, $30\sigma_y^{0\prime}$ and $E=15$ for the electron beam of KEKB.

The tails of electron beam in KEKB are extended in both the transverse and longitudinal directions, and the lifetime is mainly determined by the longitudinal and vertical apertures.

*Loss Mechanism* It was shown that a particle in a beam could be mainly lost by the following two ways: First, a particle is lost by a single random process from the core. A particle which has undergone a random process expands beyond the apertures of the accelerator.

Second, by the single random process, the oscillation amplitude of the particle grows, but still exists inside the apertures. The tail is strongly affected by a nonlinear resonance due to the beam–beam interaction. Thus, the nonlinear resonance of the beam–beam interaction can expand the particle beyond the aperture, resulting in particle loss. The second case affects tail distributions and lifetimes more than the first case.

## 5 DISCUSSION AND CONCLUSION

More simulation studies on the beam tail distributions due to rare random processes and beam–beam interaction have been carried out.

Two simplifications were employed for our simulation to be valid: The minimum cutoff values that actually determine the probability for a random process were free parameters in this simulation. The equilibrium beam distribution should not be affected by choice of this parameter. Secondly, we assumed that new macroparticles reach an equilibrium state during two transverse damping times. It was shown that these two assumptions were valid in our simulation. They made our simulation possible to simulate long-term runs.

From our studies, it has been shown that the tranverse tails in KEKB are affected more by the influence of beam–residual gas scattering for a vacuum pressure of $10^{-9}$ Torr rather than Bhabha scattering. These scatterings only contribute to a tail of large-amplitude particles and do not affect the core of the beam distribution.

Random processes influence the lifetimes as well as the tails of the beam distribution. A simulation study of the lifetime was performed as a function of the apertures. It was shown that the beam–beam bremsstrahlung and beam–residual gas scattering in KEKB are the predominant random processes leading to particle loss. The lifetime can be more greatly affected by the variances in the vertical aperture than the horizontal and energy apertures.

A new simulation method for beam tails was applied to KEKB. The events of the random processes that we considered can be divided into three categories: (1) single event which results in particle loss; (2) single event which results in the tail distribution by the transfer of a particle and (3) single event which results in the core distribution. It is shown

that at large amplitudes the lifetime is influenced by rare random processes, such as the processes of residual gas scattering and beam–beam bremsstrahlung, rather than the beam–beam interaction. This simulation showed good agreement with the solvable case. This simulation can generate tail distributions due to various random processes in the storage rings with a simple and fast method and will be helpful in understanding the beam tail distributions.

### *Acknowledgements*

I would like to thank Prof. K. Hirata and Prof. K. Yokoya for useful discussions.

### *References*

[1] Kim, Eun-San, *Part. Accel.* **56**, 249 (1997).
[2] Hirata, K., Moshammer, H. and Ruggiero, F., CERN SL-AP/90-02.
[3] Bassetti, M. and Erskine, G., CERN ISR-TH/80-06 (1980).
[4] Hirata, K. and Yokoya, K., *Part. Accel.* **39**, 147 (1992).
[5] KEKB B-Factory Design Report, KEK Report 95-7 (1995).
[6] Heilter, W., *The Quantum Theory of Radiation*, Oxford Univ. Press (1954).
[7] Chang, S.J., *Introduction to Quantum Field Theory*, World Scientific (1990).